



## Antifungal and Anti-inflammatory Effect of Punicalagin on Murine *Aspergillus fumigatus* Keratitis

Hao Lin, Qian Wang, Yawen Niu, Lingwen Gu, Liting Hu, Cui Li & Guiqiu Zhao

To cite this article: Hao Lin, Qian Wang, Yawen Niu, Lingwen Gu, Liting Hu, Cui Li & Guiqiu Zhao (2022) Antifungal and Anti-inflammatory Effect of Punicalagin on Murine *Aspergillus fumigatus* Keratitis, *Current Eye Research*, 47:4, 517-524, DOI: [10.1080/02713683.2021.2008982](https://doi.org/10.1080/02713683.2021.2008982)

To link to this article: <https://doi.org/10.1080/02713683.2021.2008982>



Published online: 27 Dec 2021.



Submit your article to this journal [↗](#)



Article views: 111



View related articles [↗](#)



View Crossmark data [↗](#)



Citing articles: 1 View citing articles [↗](#)



# Antifungal and Anti-inflammatory Effect of Punicalagin on Murine *Aspergillus fumigatus* Keratitis

Hao Lin , Qian Wang, Yawen Niu, Lingwen Gu, Liting Hu, Cui Li, and Guiqiu Zhao

Department of Ophthalmology, The Affiliated Hospital of Qingdao University, Qingdao, China

## ABSTRACT

**Purpose:** This study aimed to investigate the anti-inflammatory effect and antifungal effect of punicalagin in murine fungal keratitis.

**Methods:** We used in vitro and in vivo protocols to assess the anti-inflammatory effect and antifungal effect of punicalagin. In vitro, time kill and mycelial stain were done. In vivo, murine fungal keratitis was established and treated with PBS or PUN. Clinical scores were taken on days 1, 3, and 5 post infection. The mRNA and protein levels of inflammatory factors were detected by RT-PCR and Western blot, and the number and location of macrophages were analyzed by flow cytometry and immunofluorescence. Also, fungal plate counting was used to assess the antifungal effect. The DCFH-DA fluorescence probe detected the ROS level.

**Results:** In vitro, PUN showed activity against *A.fumigatus* (*A.F.*), with MIC90 values of 250 µg/ml, and significantly reduced *A.F.* biofilm formation ( $p < .001$ ). In vivo, the mouse fungal keratitis model after punicalagin treatment exhibited less disease, lower clinical scores ( $p < .05$ ), lower reduced macrophage infiltrate ( $p < .001$ ), and fungal load ( $p < .001$ ) than those treated with PBS. Treatment with punicalagin also reduced the mRNA expression and protein level of pro-inflammatory factors. At the cellular level, PUN significantly reduced the mRNA expression of inflammatory factors and ROS production caused by the stimulation of mycelia in RAW264.7 ( $p < .001$ ).

**Conclusions:** The results show that punicalagin is beneficial in the treatment of murine fungal keratitis. The mechanism of its anti-inflammatory effect was synthetical, including antifungal activity, an inhibitory effect of proinflammatory factor and macrophages, and anti-oxidation.

## ARTICLE HISTORY

Received 13 August 2021  
Revised 15 October 2021  
Accepted 2 November 2021

## KEYWORDS

Fungal keratitis; Punicalagin; *A.fumigatus*; mice; macrophage

## Introduction

Fungal keratitis (FK) is a severe ocular disease and one of the leading causes of corneal ulcers<sup>1</sup> and blindness.<sup>2</sup> Increased agricultural trauma, long-term antibiotic use, extended contact lens use, and the excessive use of corticosteroids increase the occurrence of this disease.<sup>3</sup> *Aspergillus fumigatus* (*A.F.*) is a common fungal pathogen that is responsible for a high proportion of fungal keratitis<sup>4,5</sup> due to its invasiveness<sup>6</sup> and the corneal inflammation it causes.<sup>7,8</sup>

Punicalagin (PUN) is the most abundant ellagitannin in pomegranate and is widely used in traditional Chinese medicine.<sup>9</sup> Previous studies have shown that PUN can play an active role in anti-inflammatory, antioxidant, anti-cancer, anti-fungal, anti-apoptosis, and anti-glycation response.<sup>10–14</sup> Despite increasing interest in PUN's capacities, there is no current literature reporting its influence on fungal keratitis. PUN has been shown to target macrophages<sup>9</sup> and inhibit oxidative stress in LPS-induced macrophages,<sup>10</sup> and previous studies suggest that it shows anti-fungal activity against the conidial and hyphal stages of dermatophytes, including *Trichophyton mentagrophytes*<sup>15</sup> and three *Candida* species.<sup>16,17</sup> Importantly, cytotoxicity assays show that PUN exhibits selectivity for fungal cells in preference to mammalian cells.<sup>15</sup>

We used the AGAR diffusion test, MIC (minimum inhibitory concentration), fluorochrome stain, and biofilm assay to observe fungi in response to PUN stimulation. In vivo studies tested whether PUN was effective in the treatment of *A.F.* induced keratitis in B6 mice. Evidence showed that PUN treatment was antifungal against *A.F.* and reduced disease by the downregulation of macrophage infiltration, fungi count, and proinflammatory molecules. Tests in RAW264.7 macrophages verified the anti-inflammatory and antioxidant activity of PUN. These results suggest that PUN may be an effective alternative for the existing treatment of *A.F.* induced keratitis.

## Method

### Mice

C57BL/6 (B6) female mice (7 weeks of age, weight 18–22 g) were purchased [the Institute of Laboratory Animal Science, Chinese Academy of Medical Sciences (CAMS)] and fed in a comfortable condition at 4/hutch. B6 mice were subjected to adaptive feeding for 1 week before the experiment. The fungal keratitis model was established on just the right eye. All animal usage complied with ARVO guidelines.

### Fungal straining

Standard *Aspergillus fumigatus* strain (no. 3.0772) was bought from the China General Microbiological Culture Collection Center. Spores collected in a sterile environment were inoculated on Sabouraud dextrose agar medium, in 28°C, 24 hours, recovery in batches then adjusted to  $1 \times 10^6$  CFU/ml. Mycelia of *A. fumigatus* were collected in 28°C for 7 days and milled to 20–40 microns for animal models or stimulate cells. The devitalized mycelia were treated with 75% alcohol, 12 hours and washed with PBS three times, and mycelia fragments were counted and adjusted to  $1 \times 10^8$  CFU/ml.

### Cell culture and *A. fumigatus* stimulation

RAW264.7 (obtained from Shanghai Chinese Academy of Sciences) murine macrophage cells were cultured in High Glucose Dulbecco's Minimal Essential Medium (DMEM, Gibco, USA) supplemented with 10% fetal bovine serum (FBS, Gibco, USA). Immortalized HCEC were cultured in DMEM-F12 (HAM, 1:1, BI). Both of them were incubated at 37°C in 5% CO<sub>2</sub>. Near 80% confluence, the cells were pre-treated with 0, 25, 50, or 100 µg/ml PUN (98% (HPLC), Sigma-Aldrich, USA) for 2 h and then incubated with *A. fumigatus* hyphae (to the final concentration of  $5 \times 10^6$  CFU/mL) in 12-well plates or 96-well plates.

### Cell counting kit-8 (CCK-8) assay

HCEC was seeded in 96-well plates at a density of  $3 \times 10^3$  cells per well in 200 µl per well. PUN was added to the medium at final concentrations of 0, 50, 100, and 200 µg/ml. Each condition was repeated six times. After culturing in a cell culture incubator for 24 h and 48 h, the plates were removed, and 10 µl of CCK-8 (MCE, New Jersey, America) was added to every well. The cells were incubated for an additional 2 h. The optical density (OD) of each well was measured by ELISA at 450 nm.<sup>18</sup>

### MIC

Serial dilutions of PUN (90 µl/well) were prepared in salouraud liquid medium, and 10 µl of spore suspension (adjusted to  $5 \times 10^4$  CFU/mL) was added to each tube and incubated at 29°C in 90% CO<sub>2</sub> for 12 hours. Visible fungal growth at each PUN concentration was examined by spectrophotometry at 570 nm. MIC was assigned as the lowest PUN concentration that inhibited visible fungal growth.

### Calcofluor white staining

Sterilized salouraud liquid medium was prepared in four Chambered cover glass (Thermo Fisher), on which cover slips were placed. The samples were prepared in duplicate for each concentration. The walls were inoculated with spore suspension, containing 5000–7500 spores. All plates were incubated at 29°C in 90% CO<sub>2</sub> for 24 hours. Then, the slides were washed three times with sterile PBS.<sup>19</sup> After air drying, each slide was stained with 0.5 mL Calcofluor white stain (Sigma) for 30 s. Then, the chambers were gently decanted and washed with PBS. After air drying, the coverslips were mounted to the chambered slide with antifade mounting medium. All specimens were observed and photographed by a fluorescence microscope (Leica).<sup>15</sup>

### Fungal keratitis models

Mice were anesthetized with chloral hydrate. Preoperative routine disinfection and towel laying were done. The 2/3 epithelium (about a diameter of 2 mm) of its right cornea was removed from the central cornea under the stereoscopic microscope. *A. fumigatus* hyphae was evenly coated on the corneal surface, and contact lenses were placed. Close their eyelids for 1 day. Randomization was used to allocate experimental mice to control and treatment groups by testers. Six successfully modeled corneas were divided into a group to ensure the accuracy of the experiment. Slit lamp photography and clinical score (the standard of clinical scoring referred to Wu et al. was expressed in Table 1)<sup>20</sup> were taken every day and animals were killed by internal decapitation after anesthetized excessively, and the eyeballs were processed according to the experimental requirements.<sup>21</sup>

### Therapy

Punicalagin eyedrop (using pasteurized PBS to dissolve punicalagin powder and mix, dilute it when it will be used) treatment was carried out four times a day and 3 µl at a time under isoflurane gas anesthesia in the PUN group. The eyes of the control group were treated with PBS eyedrops (pasteurized PBS). The time of the whole treatment process was controlled to less than 1 hour to minimize potential confounders.

### Plate count

Mice (n = 6/group/time) were euthanized at 2 days p.i, and its corner was removed into sterile HANK's balance salt solution. Each cornea was cryomilled with 500 µl of PBS with sterilized glass

**Table 1.** Visual scoring system for murine fungal keratitis.

Visual Scoring System for Murine Fungal Keratitis				
	Grade 1 (1)	Grade 2	Grade 3	Grade 4
Area of corneal opacity	1–25%	26–50%	51–75%	76–100%
Density of corneal opacity	Slight cloudiness, outline of iris and pupil discernable	Cloudy, but outline of iris and pupil remain visible	Cloudy, opacity not uniform	Uniform opacity
Surface regularity	Slight surface irregularity	Rough surface, some swelling	Significant swelling, crater or serious descemetocoele formation	Perforation or descemetocoele

The score is the sum of three terms

rod grinding by hand. Then, all grinding fluid was plated on Sabouraud solid medium and incubated at 37°C for 36 hours. Colonies were counted to reflect viable fungi surviving on the cornea.

### Real time reverse transcription-polymerase chain reaction (RT-PCR)

Normal and infected (fungi) corneas were removed at 5 days p.i. from B6 mice after PUN or PBS-treatment. The RAW 264.7 clone was stimulated by inactivated hyphae for 6 hours after PBS or PUN-pretreatment 2 hours. All samples were collected in RNAiso Plus reagent (Takara) and was rapidly quantified by spectrophotometry (Eppendorf). The protocol used has been described in our previous publications.<sup>22</sup>  $\beta$ -actin was used as an internal control. The primers used are shown in Table 2.

### Western blot

Corneas and cells were collected in radioimmunoprecipitation assay (RIPA; Solarbio) lysis buffer containing and phenylmethanesulfonyl fluoride (PMSF; Solarbio) (100:1:1). The protocol used has been described in our previous publications.<sup>22</sup> Primary antibodies against the following proteins were used: IL-1 $\beta$ (Bioss), TNF- $\alpha$ (Signaling Technology, Massachusetts, USA),  $\beta$ -actin(Elbscience). Secondary antibodies included HRP-linked anti-rabbit (Elbscience) antibodies.  $\beta$ -actin was set for a control. The immunoreactive bands were exposed with ECL reagents (Thermo Fisher Scientific, Waltham, MA, USA).<sup>22</sup>

### Flow cytometry

Mice (n = 6/group/time) were euthanized at 3 days p.i, and its corner was removed into sterile HANK's balance salt solution, and separated into individual cells after 2% liberase (sigma, USA) immersion at 37°C for 60 minutes and crushing by micro pipette tips, and stained with CD45-PEvio (1:150; Miltenyi Biotec, Bergisch Gladbach, Germany), F4/80(1:200; BioLegend, San Diego, CA, USA) for 20 minutes. Macrophages were among the CD45<sup>+</sup> cells, F4/80<sup>+</sup> cells, shown by monitoring

singular cell suspensions stained with fluorescently labeled antibodies. The data of flow cytometry was assayed on a Beckma flow cytometer and analyzed by FlowJo 10.4 software.

### Immunofluorescence staining

For tissue immunofluorescence, mouse eyes (n = 6/group /time point) were embedded in an OCT compound (Tissue-Tek; Miles, Elkhart, IN, USA), and frozen in liquid nitrogen. The protocol used here has been described in previous publications.<sup>23</sup> Primary antibodies rat anti-mouse F4/80 antibody (1:400; abcam, ab6640) was used for their respective organisms. A Cy3-conjugated goat anti-rat antibody (1:400; Bioss, Beijing, China) was used as secondary antibodies. And DAPI dihydrochloride was used for marking the nucleus. All samples were observed and photographed by fluorescence microscopy.

### Assay of the intracellular production of ROS

The production of ROS was estimated with 2', 7'-Dichlorodihydrofluorescein diacetate (DCFH-DA, MCE, China) which becomes fluorescent after oxidation to 2',7'-dichlorofluorescein (DCF). RAW264.7 clone was cultured in DMEM without FBS in 96-well plates and incubated at 37°C in 5% CO<sub>2</sub>. Near 80% confluence, the cells were incubated with *A. fumigatus* hyphae (to the final concentration of 5 × 10<sup>6</sup> CFU/mL) and 0, 25, 50 or 100  $\mu$ g/ml PUN for 6 distinct time points. After this incubation, each well was washed twice with PBS. 96-well plates were preincubated in the dark, at 25°C for clocked 0.5 h in the presence of 10  $\mu$ M DCFH-DA, then washed twice with PBS.<sup>24</sup> The samples were excited at 480 ± 30 nm and the light emitted at 580 ± 20 nm.

### Statistical analysis

The difference in clinical score between two groups was tested by the Mann-Whitney U test. For comparison of three or more groups, a one-way ANOVA followed by the Bonferroni's multiple comparison test (GraphPad Prism) was used for analysis. For each data,  $p < .05$  was considered significant and data was shown as mean ± SEM. To ensure reproducibility, all experiments were repeated at least once.<sup>25</sup>

**Table 2.** Primer list used for RT-PCR.

Gene	Genbank No.	Primer Sequence (5'-3')
$\beta$ -actin	NM-0073933	F: GAT TAC TGC TCT GGC TCC TAG C R: GAC TCA TCG TAC TCC TTG C
IL-1 $\beta$	NM-0083613	F: CGC AGCAGC ACA TCA ACA AGA GC R: TGT CCT CAT CCT AGG TCC ACG
TNF- $\alpha$	NM-0136932	F: ACC CTC ACA CTC AGA TCA TCT T R: GGT TGT CTT TGA GAT CCA TGC
MIP-2	NM-0091402	F: TGT CAA TGC CTG AAG ACC CTG CC R: AAC TTT TTG ACC GCC CTT GAG AGT GG
iNOS	NM-0109273	F: TCC TCA CTG GGA CAG CAC AGAATG R: GTG TCA TGC AAA ATC TCT CCA CTG CC
TLR 4	NM-0212972	F: CGC TTT CAC CTC TGC CTT CAC TAC AG R: ACA CTA CCA CAA CCT TCC GGC TC
CXCL 1	NM-0081763	F: TCA CCT CAA GAA CAT CCA GAG C R: ACT TGG GGA CAC CTT TTA GCA T
IL-6	NM-0311681	F: CAC AAG TCC GGA GAG GAG AC R: CAG AAT TGC CAT TGC ACA AC
IL-10	NM-0105482	F: TGC TAA CCG ACT CCT AGG AC R: CCT TGA TTT CTG GGC CAT GCT C

### Result

The disk diffusion test performed drug sensitivity testing. The inhibition zone diameter of amphotericin B was larger when combined with PUN, indicating the latter's anti-fungal synergy. MIC showed PUN can inhibit the growth of *A.F.* at 31.25  $\mu$ g /ml, and prevented 90% of *A.F.* growth at 500  $\mu$ g /ml (Figure 1b,  $p < .001$ ,  $p < .001$ ,  $p < .001$ ,  $p < .001$  and  $p < .001$ , respectively). Calcofluor White stain, a non-specific fluorescent dye that binds to cellulose and chitosan in cell wall, was used to observe fungi growth in this study. Fluorescent microscopy images showed fungi were nearly invisible when treated with different PUN concentrations, and their branches were reduced (Figure 1b). Fungal biofilm was stained with crystal violet, and the absorbance of the eluate at OD570nm decreased with increasing concentrations of PUN, indicating that the

formation of *A.F.* biofilm was inhibited (Figure 1c,  $p < .001$ , and  $p < .001$ , respectively). To validate the antifungal effect in vivo, the grinding fluid of infected corneas was plated and grown on Sabouraud solid medium on day 3 (Figure 2e). This showed that the number of fungi in the PUN400 group was significantly lower than in the PBS group (Figure 2f,  $p < .001$ , and  $p < .001$ , respectively).

We used the cell counting kit-8 (CCK-8) to test cell viability for different concentrations of PUN in HCECs and murine macrophages (RAW264.7 cells). PUN showed no significant cytotoxic effect at 0 to 400  $\mu\text{g}/\text{mL}$  for 48 hours (Figure 2a,b). RT-PCR was used to evaluate the mRNA expression in macrophages with pretreatment of PUN. Data showed that *A.F.*

stimulation could significantly increase the levels of mRNA expression of inflammatory factors including IL-1 $\beta$  (Figure 2c,  $p < .001$ ), IL-6 (Figure 2d,  $p < .001$ ), IL-10 (Figure 2e,  $p < .001$ ), TNF- $\alpha$  (Figure 2f,  $p < .001$ ), MIP-2 (Figure 2h,  $p < .001$ ), and TLR 4 (Figure 2g,  $p < .001$ ). With an increase in the concentration of PUN, the *A.F.*-induced upregulation of mRNA levels was inhibited (Figure 2c,  $p < .001$ ,  $p < .001$  and  $p < .001$ , respectively; Figure 2d,  $p < .001$ ,  $p < .001$ , and  $p < .001$ , respectively; Figure 2e,  $p < .001$ ,  $p < .001$  and  $p < .001$ , respectively; Figure 2f,  $p < .001$ ,  $p < .001$  and  $p < .001$ , respectively; Figure 2g,  $p < .001$ ,  $p < .001$  and  $p < .001$ , respectively; Figure 2h,  $p < .001$ ,  $p < .001$  and  $p < .001$ , respectively). ROS production

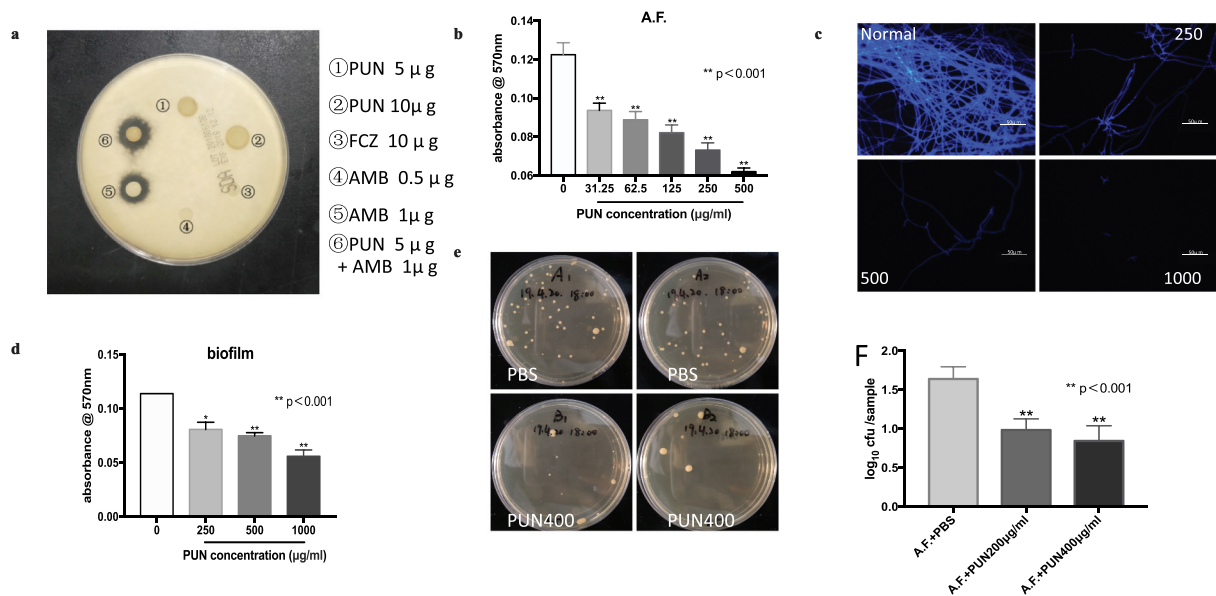


**Figure 1.** [(a)–(f)] Antifungal effect of PUN. The MIC<sub>50</sub> of PUN was 125  $\mu\text{g}/\text{ml}$ , and the MIC<sub>90</sub> was 500  $\mu\text{g}/\text{ml}$  (B). Fluorescent staining of *A.F.* suggested the fungal number fell when cultured with PUN (C). Biofilm formation was inhibited significantly by PUN at more than 250  $\mu\text{g}/\text{ml}$  in vitro compared with PBS treatment, which was demonstrated by the absorbance values of crystal violet released from biofilm (D). A spiral and surface spread plate method was used to count viable *A.F.* on the cornea (E), and the results revealed that PUN significantly decreased the viable count of fungi ( $n = 6/\text{group}/\text{time}$ ) (F). Data are mean  $\pm$  SEM analyzed using one-way ANOVA.

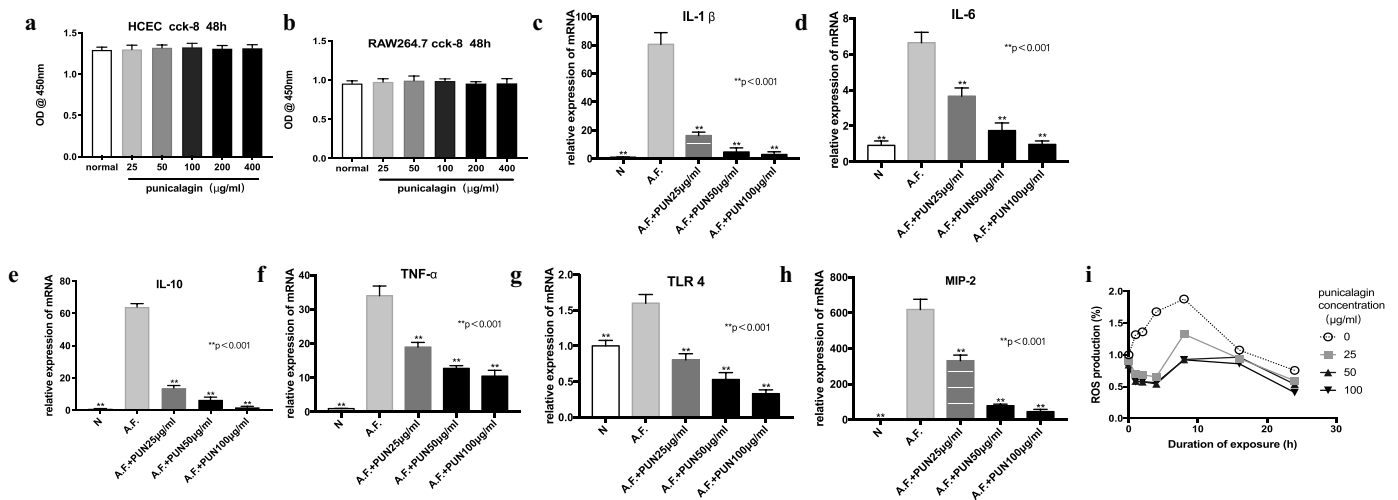


**Figure 2.** [(a)–(i)] Effect of PUN on the function of cell lines. The CCK-8 cell viability assay was performed on HCECs and RAW264.7 cells at 48 hours using different concentrations of PUN (0 ~ 400  $\mu\text{g}/\text{mL}$ ) (A, B). After PUN-pretreatment for 2 hours with or without *A.F.* stimulation for 8 hours, relative mRNA levels of IL-1 $\beta$  (C), IL-6 (D), IL-10 (E), TNF- $\alpha$  (F), TLR4 (G), and MIP-2 (H) were extracted from the cell lines ( $n = 6/\text{group}/\text{time}$ ). With *A.F.* stimulation, the level of mRNA of these cytokines increased. After *A.F.* stimulation and PUN-treatment, ROS first decreased and then increased. Increasing concentrations of PUN caused ROS production to decrease (I). Data are mean  $\pm$  SEM analyzed using one-way ANOVA.

was determined by a DCFH-DA fluorescence probe in macrophages at seven distinct time points (0 h, 1 h, 2 h, 4h, 8 h, 16 h, and 24 h). Without PUN-treatment, *A.F.* hyphae stimulated macrophages to produce ROS at the first 8 hours before ROS levels decreased. After different concentrations of PUN-treatment were used, the ROS level first decreased and then increased. At the same time point, with the increase in PUN, the *A.F.*-induced upregulation of ROS levels decreased (Figure 2i), indicating the anti-inflammatory and antioxidant effect of PUN in macrophages.

To illustrate PUN's disease response, we used a slit lamp to take photographs of the PBS and PUN400 groups on days 1, 3, and 5 post-infection (p.i.). (Figure 3a). Photographs showed that the clinical score was significantly lower in the PUN group than that in the PBS group (Figure 3b, ns,  $p < .05$  and  $p < .001$ , respectively). RT-PCR data showed that on day 5 p.i., treatment with 200  $\mu\text{g}/\text{ml}$  PUN and 400  $\mu\text{g}/\text{ml}$  PUN drops four time per day significantly inhibited *A. fumigatus*-induced upregulation of inflammatory factors including IL-1 $\beta$  (Figure 3c,  $p < .001$  and  $p < .001$ , respectively), IL-6 (Figure 3d,  $p < .001$  and  $p < .001$ , respectively), TNF- $\alpha$  (Figure 3e,  $p < .05$  and  $p < .001$ , respectively), CXCL1 (Figure 3f,  $p < .001$  and  $p < .001$ , respectively), and in particular, iNOS (Figure 3g, ns and  $p < .05$ , respectively). To confirm these data, IL-1 $\beta$  and TNF- $\alpha$  protein were tested, and the results of Western blot confirmed the RT-PCR results (Figure 3i,  $p < .05$  and  $p < .001$ ; Figure 3h,  $p < .001$  and  $p < .001$ , respectively).

We used flow cytometry and indirect immunofluorescence staining to explore the effect of PUN on macrophage infiltration. The number and proportion of macrophages were tested by F4/80 stainings combined with fluorescent antibody labeling and flow cytometry (Figure 4a). Flow cytometry data showed that treatment with PUN significantly reduced the number and proportion of macrophages in infected corneas at 3 days p.i. (Figure 4b,  $p < .001$  and  $p < .001$ , respectively; 4 C,  $p < .05$  and  $p < .001$ , respectively). Indirect-

immunofluorescence staining demonstrated that the macrophage (red) number was significantly reduced when treated with 200  $\mu\text{g}/\text{ml}$  PUN at 3 days p.i., and the depth of infiltration was shallower than that in the PBS group (Figure 4d).

## Discussion

Filamentous fungi are a common cause of visual impairment and blindness worldwide,<sup>1</sup> especially in developing countries.<sup>2</sup> While the most common treatment of fungal keratitis is the application of antifungal medicine,<sup>8,26</sup> due to the increase in fungal resistance, the use of pharmaceutical treatment alone is not ideal.<sup>27</sup> PUN is a hydrolyzable tannin recognized to have both antifungal and anti-inflammatory functions.<sup>28</sup> Our study showed that PUN had antifungal activity against *A.F.* in vitro and in vivo, indicating the protective potential of PUN in clinical antifungal therapy.

Calcofluor white stain showed that the branches and growth rate of *A.F.* decreased with increasing PUN.<sup>15</sup> Hydrolyzable tannins (HT), of which PUN is the most bioactive, have antifungal activity and help exert the effect of fluconazole.<sup>28,29</sup> The effect of PUN on *C. albicans* and *C. krusei* was examined by scanning and transmission electron microscopy and showed changes in fungal morphology and structure.<sup>17</sup> Research has shown that PUNs act similarly to other HTs by having the protein-binding capability and forming irreversible interactions with nucleophilic amino acids leading to protein deactivation and loss of function.<sup>30</sup> Proteins existing in surface-exposed adhesions, enzymes, receptors, and cell wall polypeptides are probable targets in fungi.<sup>28,31</sup> Our research also shows that PUN significantly inhibits biofilm formation, which plays a major role in fungal adhesion, growth, pathogenicity, resistance, and virulence.<sup>32,33</sup> The inhibitory effect of PUN against *S. aureus*, *Escherichia coli*, and *Candida albicans* may also be related to it inducing protein precipitation and enzyme inactivation.<sup>34-36</sup>

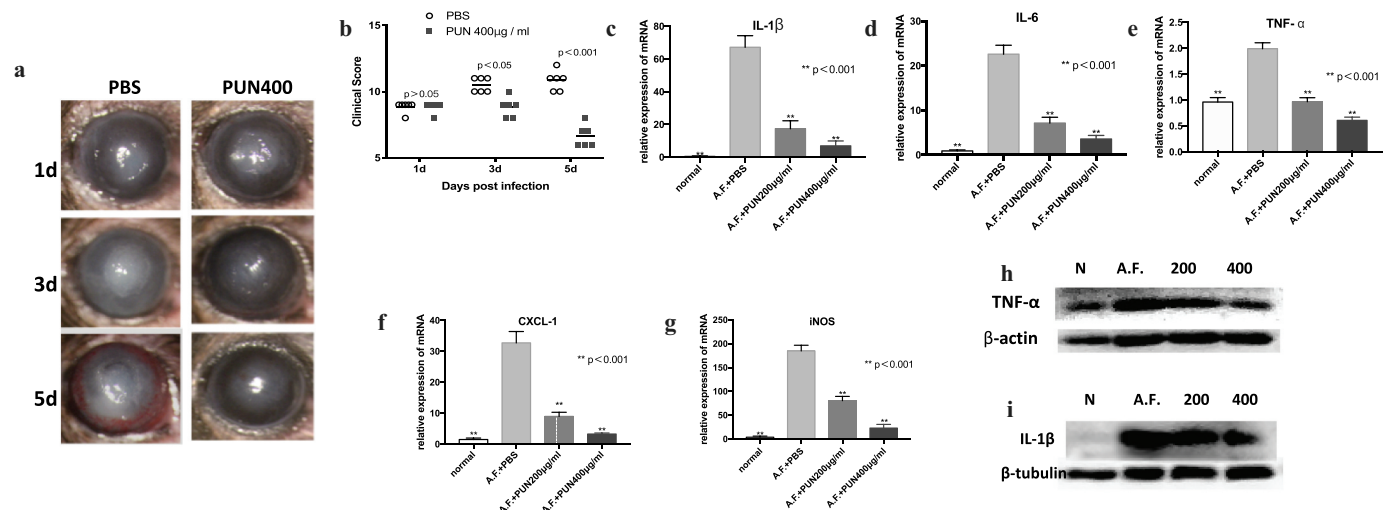


**Figure 3.** [(a)–(i)] Inflammatory response after PUN-treatment in test corneas. Photographs were taken with a slit lamp of PBS and 400  $\mu\text{g}/\text{ml}$  PUN treated mice on days 1, 3, and 5 post infection (p.i.) confirmed reduced opacity after PUN treatment (A) and clinical scores were reduced significantly on days 3 and 5 p.i. in PUN vs. PBS treated mice ( $n = 6/\text{group}$ ) (B). Data are mean  $\pm$  SEM analyzed using a two tailed student t test. Corneal mRNA levels of IL-1 $\beta$ (C), IL-6 (D), TNF- $\alpha$ (E), CXCL1(F), and iNOS (G) were reduced significantly after PUN treatment. Corneal protein expression levels of IL-1 $\beta$ (I) and TNF- $\alpha$ (H) were also significantly reduced at 5 days p.i. Protein and mRNA levels were also lower in the 400 groups compared with the 200 groups. Data are mean  $\pm$  SEM analyzed  $\pm$  SEM analyzed using one-way ANOVA ( $n = 6/\text{group}/\text{time}$ ).

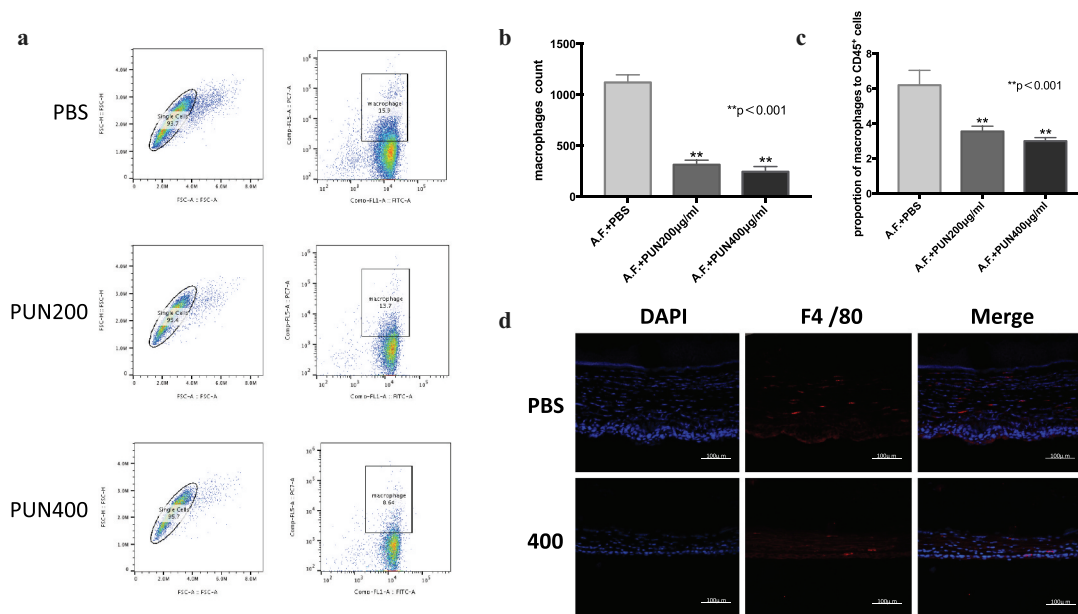


**Figure 4.** [(a)–(d)] Effect of PUN on corneal macrophages. Corneal macrophages analyzed by flow cytometry (A) in cornea treated with 200  $\mu\text{g/ml}$  or 400  $\mu\text{g/ml}$  PUN decreased in number and proportion compared with the PBS group at 3 days p.i. (B, C) ( $n = 5/\text{group/time}$ ). Red fluorescence represented macrophages and DAPI (blue) was used to stain nuclei. Indirect immunofluorescence staining showed reduced macrophage numbers in corneas treated with 400  $\mu\text{g/ml}$  PUN (D). Data are mean  $\pm$  SEM analyzed using one-way ANOVA.

Our data suggested that classical inflammatory factors in fungal keratitis, such as mRNA and protein levels, were also significantly reduced after PUN treatment. At the same time, inflammation is a double-edged sword,<sup>37</sup> and when in excess, it may lead to damage of corneal tissue and exacerbation of the clinical manifestations of fungal keratitis.<sup>38,39</sup> PUN has a powerful anti-inflammatory effect and is widely used in Chinese medicine.<sup>40</sup> Our results support previous studies that have shown that PUN plays an anti-inflammatory role in dental tissue, ex vivo skin, and in vitro models of the human intestine, bovine endometrial epithelial cells,<sup>37,41–43</sup> and provide evidence that PUN treatment is beneficial to fungal keratitis outcomes.

Our previous studies have confirmed the important role of macrophages in the acute onset of acute inflammation.<sup>23</sup> Our FCM and immunofluorescence data revealed that PUN reduced the number and proportion of macrophages in treated corneas and limited their infiltration depth. Experiments on RAW264.7 were used to explore the effects of PUN on macrophages further. Previous studies have shown that PUN can affect macrophages' secretion stimulated by LPS,<sup>40,44,45</sup> but not by fungi. We found that PUN can limit inflammation by decreasing the essential inflammatory factor and ROS levels stimulated by fungi.<sup>46–51</sup> PUN's oxidative stress of human epidermal keratinocytes, foam cells, and NIH3T3 cells is also reduced.<sup>46–54</sup> Studies by Kim, Y have shown that PUN can inhibit LPS-induced A $\beta$ 1-42 generation through down-regulation of APP and BACE1 expression and directly bind to NF- $\kappa$ B subunit p50 on neuro inflammation.<sup>55</sup> Finally, PUN can upregulate the Nrf2-mediated pathway and enhance HO-1 expression, leading to a decrease in ROS generation and NO overproduction,<sup>10</sup> which indicates that PUN may exhibit its anti-inflammatory effects via mitochondrial function. However, further study is required to determine its exact anti-inflammatory mechanisms.

## Conclusion

The results of this study confirm that PUN reduces fungal keratitis in mice. Its action against *A.F.* and its ability to inhibit inflammation by macrophages had also been demonstrated. These results will help provide new ideas for the treatment of *Aspergillus fumigatus* keratitis.

## Data availability statement

The authors confirm that the data supporting the findings of this study are available within the article or its supplementary materials.

Other data that support the findings of this study are available from the corresponding author, Guiqiu Zhao, upon reasonable request.

## Disclosure statement

No potential conflict of interest was reported by the author(s).

## Funding

This work was supported by the National Natural Science Foundation of China [no. 89100824].

## ORCID

Hao Lin  <http://orcid.org/0000-0001-8630-5566>

## References

1. Leal SM, Vareechon C, Cowden S, Cobb BA, Latgé J-P, Momany M, Pearlman E. Fungal antioxidant pathways promote survival against neutrophils during infection. *J Clin Invest.* 2012;122:2482–98. doi:10.1172/JCI63239.

2. Huang JF, Zhong J, Chen GP, Lin ZT, Deng Y, Liu YL, Cao PY, Wang B, Wei Y, Wu T, et al. A hydrogel-based hybrid theranostic contact lens for fungal keratitis. *ACS Nano*. 2016;10:6464–73. doi:10.1021/acsnano.6b00601.
3. Niu Y, Zhao G, Li C, Lin J, Jiang N, Che C, Zhang J, Xu Q. *Aspergillus fumigatus* increased PAR-2 expression and elevated proinflammatory cytokines expression through the pathway of PAR-2/ERK1/2 in cornea. *Invest Ophthalmol Vis Sci*. 2018;59:166–75. doi:10.1167/iovs.17-21887.
4. De Luca A, Iannitti RG, Bozza S, Beau R, Casagrande A, D'Angelo C, Moretti S, Cunha C, Giovannini G, Massi-Benedetti C, et al. CD4(+) T cell vaccination overcomes defective cross-presentation of fungal antigens in a mouse model of chronic granulomatous disease. *J Clin Invest*. 2012;122:1816–31. doi:10.1172/JCI60862.
5. Levitz SM, Leal SM, Cowden S, Hsia Y-C, Ghannoum MA, Momany M, Pearlman E. Distinct roles for Dectin-1 and TLR4 in the pathogenesis of *aspergillus fumigatus* keratitis. *PLoS Pathog*. 2010;6:e1000976. doi:10.1371/journal.ppat.1000976.
6. Orciuolo E, Stanzani M, Canestraro M, Galimberti S, Carulli G, Lewis R, Petrini M, Komanduri KV. Effects of *Aspergillus fumigatus* gliotoxin and methylprednisolone on human neutrophils: implications for the pathogenesis of invasive aspergillosis. *J Leukoc Biol*. 2007;82:839–48. doi:10.1189/jlb.0207090.
7. Bochud PY, Chien JW, Marr KA, Leisenring WM, Upton A, Janer M, Rodriguez SD, Li S, Hansen JA, Zhao LP, et al. Toll-like receptor 4 polymorphisms and aspergillosis in stem-cell transplantation. *N Engl J Med*. 2008;359:1766–77. doi:10.1056/NEJMoa0802629.
8. Thomas PA. Current perspectives on ophthalmic mycoses. *Clin Microbiol Rev*. 2003;16:730–97. doi:10.1128/CMR.16.4.730-797.2003.
9. Xu X, Guo Y, Zhao J, He S, Wang Y, Lin Y, Wang N, Liu Q. Punicalagin, a PTP1B inhibitor, induces M2c phenotype polarization via up-regulation of HO-1 in murine macrophages. *Free Radic Biol Med*. 2017;110:408–20. doi:10.1016/j.freeradbiomed.2017.06.014.
10. Xu Q, Zhao G, Lin J, Wang Q, Hu L, Jiang Z. Role of Dectin-1 in the innate immune response of rat corneal epithelial cells to *Aspergillus fumigatus*. *BMC Ophthalmol*. 2015;15:126. doi:10.1186/s12886-015-0112-1.
11. Cao K, Xu J, Pu W, Dong Z, Sun L, Zang W, Gao F, Zhang Y, Feng Z, Liu J. Punicalagin, an active component in pomegranate, ameliorates cardiac mitochondrial impairment in obese rats via AMPK activation. *Sci Rep*. 2015;5:14014. doi:10.1038/srep14014.
12. Zou X, Yan C, Shi Y, Cao K, Xu J, Wang X, Chen C, Luo C, Li Y, Gao J, et al. Mitochondrial dysfunction in obesity-associated non-alcoholic fatty liver disease: the protective effects of pomegranate with its active component punicalagin. *Antioxid Redox Signal*. 2014;21:1557–70. doi:10.1089/ars.2013.5538.
13. Kumagai Y, Nakatani S, Onodera H, Nagatomo A, Nishida N, Matsuura Y, Kobata K, Wada M. Anti-Glycation effects of pomegranate (*Punica granatum L.*) fruit extract and its components in vivo and in vitro. *J Agric Food Chem*. 2015;63:7760–64. doi:10.1021/acs.jafc.5b02766.
14. Wang Y, Chen B, Longtine MS, Nelson DM. Punicalagin promotes autophagy to protect primary human syncytiotrophoblasts from apoptosis. *Reproduction*. 2016;151:97–104. doi:10.1530/REP-15-0287.
15. Foss SR, Nakamura CV, Ueda-Nakamura T, Cortez DA, Endo EH, Dias Filho BP. Antifungal activity of pomegranate peel extract and isolated compound punicalagin against dermatophytes. *Ann Clin Microbiol Antimicrob*. 2014;13:32. doi:10.1186/s12941-014-0032-6.
16. Liu M, Katerere DR, Gray AI, Seidel V. Phytochemical and antifungal studies on terminalia mollis and terminalia brachystemma. *Fitoterapia*. 2009;80:369–73. doi:10.1016/j.fitote.2009.05.006.
17. Anibal PC. Antifungal activity of the ethanolic extracts of *Punica granatum L.* and evaluation of the morphological and structural modifications of its compounds upon the cells of *Candida* spp. *Braz J Microbiol*. 2013;44:839–48. doi:10.1590/S1517-83822013005000060.
18. Zhou Y, Lin J, Peng X, Li C, Zhang J, Wang Q, Zhu G, You J, Zhao G. The role of netrin-1 in the mouse cornea during *Aspergillus fumigatus* infection. *Int Immunopharmacol*. 2019;71:372–81. doi:10.1016/j.intimp.2019.03.047.
19. Peng X, Ekanayaka S, McClellan S, Barrett R, Vistisen K, Hazlett L. Characterization of three ocular clinical isolates of *P. aeruginosa*: viability, biofilm formation, adherence, infectivity, and effects of glycyrrhizin. *Pathogens*. 2017;6:52. doi:10.3390/pathogens6040052.
20. Wu TG, Wilhelmus KR, Mitchell BM. Experimental keratomycosis in a mouse model. *Invest Ophthalmol Vis Sci*. 2003;44:210–16. doi:10.1167/iovs.02-0446.
21. You J, Lin J, Zhou YF, Peng XD, He H, Li C, Zhu GQ, Zhao XQ, Zhao GQ. Role of the IL-33/ST2/p38 signaling pathway in the immune response of corneal epithelial cells to *Aspergillus fumigatus* infection. *Int J Ophthalmol*. 2019;12:549–56. doi:10.18240/ijo.2019.04.04.
22. Jiang JQ, Li C, Cui CX, Ma YN, Zhao GQ, Peng XD, Xu Q, Wang Q, Zhu GQ, Li CY. Inhibition of LOX-1 alleviates the proinflammatory effects of high-mobility group box 1 in *Aspergillus fumigatus* keratitis. *Int J Ophthalmol*. 2019;12:898–903. doi:10.18240/ijo.2019.06.03.
23. Sun Q, Li C, Lin J, Peng X, Wang Q, Jiang N, Xu Q, Zhao G. Celastrol ameliorates *Aspergillus fumigatus* keratitis via inhibiting LOX-1. *Int Immunopharmacol*. 2019;70:101–09. doi:10.1016/j.intimp.2019.02.017.
24. Fontanils U, Seil M, Pochet S, El Ouaili M, Garcia-Marcos M, Dehaye JP, Marino A. Stimulation by P2X7 receptors of calcium-dependent production of reactive oxygen species (ROS) in rat submandibular glands. *Biochimica Et Biophysica Acta (BBA) - Gen Subjects*. 2010;1800:1183–91. doi:10.1016/j.bbagen.2010.07.007.
25. Sae XP, McClellan SA, Barrett RP, Vistisen K. Effects of glycyrrhizin on a drug resistant isolate of *Pseudomonas aeruginosa*. *EC Ophthalmol*. 2018;9(5): 265–280.
26. Jeng BH. Challenges in the management of fungal keratitis. *JAMA Ophthalmol*. 2017;135:525–26. doi:10.1001/jamaophthalmol.2017.0722.
27. Bullock JD, Elder BL, Warwar RE, Snyder SA, Sizemore IE. Mechanism of drug failure in fusarium keratitis, 2004–2006. *N Engl J Med*. 2014;370:88–89. doi:10.1056/NEJMc1304053.
28. Glazer I, Masaphy S, Marciano P, Bar-Ilan I, Holland D, Kerem Z, Amir R. Partial identification of antifungal compounds from *Punica granatum* peel extracts. *J Agric Food Chem*. 2012;60:4841–48. doi:10.1021/jf300330y.
29. Endo EH, Cortez DA, Ueda-Nakamura T, Nakamura CV, Dias Filho BP. Potent antifungal activity of extracts and pure compound isolated from pomegranate peels and synergism with fluconazole against *Candida albicans*. *Res Microbiol*. 2010;161:534–40. doi:10.1016/j.resmic.2010.05.002.
30. Jacob MR, Walker LA. Natural products and antifungal drug discovery. *Methods Mol Med*. 2005;118:83–109. doi:10.1385/1-59259-943-5:083.
31. Lin LT, Chen TY, Chung CY, Noyce RS, Grindley TB, McCormick C, Lin TC, Wang GH, Lin CC, Richardson CD. Hydrolyzable tannins (chebulagic acid and punicalagin) target viral glycoprotein-glycosaminoglycan in interactions to inhibit herpes simplex virus 1 entry and cell-to-cell spread. *J Virol*. 2011;85:4386–98. doi:10.1128/JVI.01492-10.
32. Loussert C, Schmitt C, Prevost MC, Balloy V, Fadel E, Philippe B, Kauffmann-Lacroix C, Latge JP, Beauvais A. In vivo biofilm composition of *Aspergillus fumigatus*. *Cell Microbiol*. 2010;12:405–10. doi:10.1111/j.1462-5822.2009.01409.x.
33. Gravelat FN, Ejzykowicz DE, Chiang LY, Chabot JC, Urb M, Macdonald KD, Al-Bader N, Filler SG, Sheppard DC. *Aspergillus fumigatus* MedA governs adherence, host cell interactions and virulence. *Cell Microbiol*. 2010;12:473–88. doi:10.1111/j.1462-5822.2009.01408.x.
34. Xu Y, Shi C, Wu Q, Zheng Z, Liu P, Li G, Peng X, Xia X. Antimicrobial activity of punicalagin against *Staphylococcus aureus* and its effect on biofilm formation. *Foodborne Pathog Dis*. 2017;14:282–87. doi:10.1089/fpd.2016.2226.
35. Bakkiyaraj D, Nandhini JR, Malathy B, Pandian SK. The anti-biofilm potential of pomegranate (*Punica granatum L.*) extract against human bacterial and fungal pathogens. *Biofouling*. 2013;29:929–37. doi:10.1080/08927014.2013.820825.



36. Liu Y, Gallardo-Moreno AM, Pinzon-Arango PA, Reynolds Y, Rodriguez G, Camesano TA. Cranberry changes the physicochemical surface properties of *E. coli* and adhesion with uroepithelial cells. *Coll Surf B Biointerfaces*. 2008;65:35–42. doi:10.1016/j.colsurfb.2008.02.012.
37. Cooper B, Islam N, Xu Y, Beard HS, Garrett WM, Gu G, Nou X. Quantitative proteomic analysis of staphylococcus aureus treated with punicalagin, a natural antibiotic from pomegranate that disrupts iron homeostasis and induces SOS. *Proteomics*. 2018;18:e1700461. doi:10.1002/pmic.201700461.
38. Keay LJ, Gower EW, Iovieno A, Oechsler RA, Alfonso EC, Matoba A, Colby K, Tuli SS, Hammersmith K, Cavanagh D, et al. Clinical and microbiological characteristics of fungal keratitis in the United States, 2001–2007: a multicenter study. *Ophthalmology*. 2011;118:920–26. doi:10.1016/j.ophtha.2010.09.011.
39. Zhong J, Huang W, Deng Q, Wu M, Jiang H, Lin X, Sun Y, Huang X, Yuan J. Inhibition of TREM-1 and Dectin-1 Alleviates the severity of fungal keratitis by modulating innate immune responses. *PLoS One*. 2016;11:e0150114. doi:10.1371/journal.pone.0150114.
40. BenSaad LA, Kim KH, Quah CC, Kim WR, Shahimi M. Anti-inflammatory potential of ellagic acid, gallic acid and punicalagin A&B isolated from *Punica granatum*. *BMC Complement Altern Med*. 2017;17:47. doi:10.1186/s12906-017-1555-0.
41. Houston DM, Bugert J, Denyer SP, Heard CM. Anti-inflammatory activity of *Punica granatum* L. (Pomegranate) rind extracts applied topically to ex vivo skin. *Eur J Pharm Biopharm*. 2017;112:30–37. doi:10.1016/j.ejpb.2016.11.014.
42. Hollebeeck S, Winand J, Herent MF, During A, Leclercq J, Larondelle Y, Schneider YJ. Anti-inflammatory effects of pomegranate (*Punica granatum* L.) husk ellagitannins in Caco-2 cells, an in vitro model of human intestine. *Food Funct*. 2012;3:875–85. doi:10.1039/c2fo10258g.
43. Lyu A, Chen JJ, Wang HC, Yu XH, Zhang ZC, Gong P, Jiang LS, Liu FH. Punicalagin protects bovine endometrial epithelial cells against lipopolysaccharide-induced inflammatory injury. *J Zhejiang Univ Sci B*. 2017;18:481–91. doi:10.1631/jzus.B1600224.
44. Xu X, Li H, Hou X, Li D, He S, Wan C, Yin P, Liu M, Liu F, Xu J. Punicalagin induces Nrf2/HO-1 expression via upregulation of PI3K/AKT pathway and inhibits LPS-induced oxidative stress in RAW264.7 macrophages. *Mediators Inflamm*. 2015;2015:380218. doi:10.1155/2015/380218.
45. Xu X, Yin P, Wan C, Chong X, Liu M, Cheng P, Chen J, Liu F, Xu J. Punicalagin inhibits inflammation in LPS-induced RAW264.7 macrophages via the suppression of TLR4-mediated MAPKs and NF- $\kappa$ B activation. *Inflammation*. 2014;37:956–65. doi:10.1007/s10753-014-9816-2.
46. Taylor PR, Roy S, Leal SM, Sun Y, Howell SJ, Cobb BA, Li X, Pearlman E. Activation of neutrophils by autocrine IL-17A-IL-17RC interactions during fungal infection is regulated by IL-6, IL-23, ROR $\delta$  and dectin-2. *Nat Immunol*. 2014;15:143–51. doi:10.1038/ni.2797.
47. Li N, Che CY, Hu LT, Lin J, Wang Q, Zhao GQ. Effects of COX-2 inhibitor NS-398 on IL-10 expression in rat fungal keratitis. *Int J Ophthalmol*. 2011;4:165–69. doi:10.3980/j.2222-3959.2011.02.11.
48. Santacruz C, Linares M, Garfias Y, Loustaunau LM, Pavon L, Perez-Tapia SM, Jimenez-Martinez MC. Expression of IL-8, IL-6 and IL-1 $\beta$  in tears as a main characteristic of the immune response in human microbial keratitis. *Int J Mol Sci*. 2015;16:4850–64. doi:10.3390/ijms16034850.
49. Dong C, Yang MG. Inhibition of matrix metalloproteinase 9 attenuated *Candida albicans* induced inflammation in mouse cornea. *Cell Mol Biol (Noisy-le-grand)*. 2016;62:79–83. doi:10.14715/cmb/2016.62.12.14.
50. Tang Q, Che C, Lin J, He H, Zhao W, Lv L, Zhao G. Maresin1 regulates neutrophil recruitment and IL-10 expression in *Aspergillus fumigatus* keratitis. *Int Immunopharmacol*. 2019;69:103–08. doi:10.1016/j.intimp.2019.01.032.
51. Cheng M, Lin J, Li C, Zhao W, Yang H, Lv L, Che C. Wedelolactone suppresses IL-1 $\beta$  maturation and neutrophil infiltration in *Aspergillus fumigatus* keratitis. *Int Immunopharmacol*. 2019;73:17–22. doi:10.1016/j.intimp.2019.04.050.
52. Chen PS, Li JH. Chemopreventive effect of punicalagin, a novel tannin component isolated from *Terminalia catappa*, on H-ras-transformed NIH3T3 cells. *Toxicol Lett*. 2006;163:44–53. doi:10.1016/j.toxlet.2005.09.026.
53. Rosenblat M, Volkova N, Aviram M. Pomegranate phytosterol (beta-sitosterol) and polyphenolic antioxidant (punicalagin) addition to statin, significantly protected against macrophage foam cells formation. *Atherosclerosis*. 2013;226:110–17. doi:10.1016/j.atherosclerosis.2012.10.054.
54. Seok JK, Lee JW, Kim YM, Boo YC. Punicalagin and (-)-Epigallocatechin-3-Gallate rescue cell viability and attenuate inflammatory responses of human epidermal keratinocytes exposed to airborne particulate matter PM10. *Skin Pharmacol Physiol*. 2018;31:134–43. doi:10.1159/000487400.
55. Kim YE, Hwang CJ, Lee HP, Kim CS, Son DJ, Ham YW, Hellstrom M, Han SB, Kim HS, Park EK, et al. Inhibitory effect of punicalagin on lipopolysaccharide-induced neuroinflammation, oxidative stress and memory impairment via inhibition of nuclear factor-kappaB. *Neuropharmacology*. 2017;117:21–32.